Pressure-independent through-plane electrical conductivity measurements of highly filled conductive polymer composites

Larsen, Thomas; Larsen, Tom; Andreasen, Søren Juhl; Christiansen, Jesper De C.

Published in:
International Journal of Hydrogen Energy

DOI (link to publication from Publisher):
10.1016/j.ijhydene.2022.11.318

Publication date:
2023

Document Version
Publisher's PDF, also known as Version of record

Available online at www.sciencedirect.com

ScienceDirect

journal homepage: www.elsevier.com/locate/he

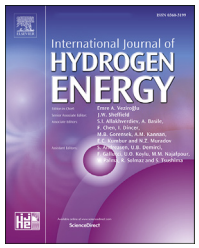

Short Communication

Pressure-independent through-plane electrical conductivity measurements of highly filled conductive polymer composites

Thomas Larsen [a,b], *Tom Larsen* [b], *Søren J. Andreasen* [b], *Jesper D.C. Christiansen* [a,*]

[a] *Aalborg University, Department of Materials and Production, Fibigerstræde 16, Aalborg, 9000, Denmark*
[b] *Advent Technologies A/S, Lyngvej 8, Aalborg, 9000, Denmark*

HIGHLIGHTS

- Eutectic gallium-indium (EGaIn) as liquid metal electrical contacts.
- EGaIn contacts for pressure-independent through-plane electrical conductivity.
- Compared to carbon paper contacts, EGaIn reduces contact resistance.

ARTICLE INFO

Article history:
Received 22 August 2022
Received in revised form
8 November 2022
Accepted 28 November 2022
Available online 31 December 2022

Keywords:
Composite
Fuel cell
Contact resistance
Resistivity
Surface roughness

ABSTRACT

Highly filled conductive polymer composites (CPCs) are widely used in applications such as bipolar plate materials for polymer electrolyte membrane fuel cells and redox flow batteries, electromagnetic interference shielding and sensors due to their useful electrical properties. A common method for determining through-plane electrical conductivities (σ_{tp}) of such highly filled CPCs applies a conductive carbon paper between electrodes and sample with application of external pressure to improve electrical contact. We show the pressure-dependence of the measured σ_{tp} can be eliminated by using a liquid metal such as the gallium-indium eutectic alloy (EGaIn) as contact material. Results indicate that EGaIn reduces contact resistance and causes a four times larger σ_{tp} compared to measurements with carbon paper contacts and a pressure of 20 bar.

Introduction

Highly filled conductive polymer composites (CPCs) are widely used for applications requiring high electrical conductivities such as bipolar plates in redox flow batteries and polymer electrolyte membrane fuel cell (PEMFC) systems in transportation, stationary applications and portable communication [1–4]. Such CPCs typically include high contents of conductive carbon fillers such as graphite and carbon black to achieve high electrical conductivities [5,6].

* *Corresponding author.*
E-mail address: jc@mp.aau.dk (J.D.C. Christiansen).

https://doi.org/10.1016/j.ijhydene.2022.11.318

Measurements of electrical conductivities, both in-plane (σ_{ip}) and through-plane (σ_{tp}), have been used in the development and optimization of highly filled CPCs [2,4,7–10]. Such composites with oriented and anisotropic conductive fillers are known to display a σ_{ip}/σ_{tp} anisotropy depending on the type of filler, their morphology and orientation, e.g., due to the processing method in the composite [2,11–13]. Comprehensive reviews exist which compare σ_{ip} and σ_{tp} of numerous composites, aimed for PEMFC bipolar plate applications, with different matrices, filler types and content, as well as fabrication processes [5,6,11,12]. In such applications, σ_{tp} is considered critical since the current travels in the through-plane direction in an operating fuel cell [13]. Thus, it is important to accurately determine both σ_{ip} and σ_{tp}.

In samples of relatively high electrical conductivities, in-plane electrical conductivities are commonly evaluated using a four-point probe technique to exclude contact resistances [14]; on the microscale, surfaces are rough and constitute asperities which form discrete points of contact between contacting bodies, thus constricting electrical current and resulting in a contact resistance [15]. The four-point probe method may also be applied to evaluate σ_{tp}, yet relatively thick samples are required for the spacing of probes [16]. Alternatively, a two-point probe technique may be used, although the method has a significant contribution from contact resistances and thus works best for low electrical conductivity samples. Yet, a transmission line method (TLM), based on extrapolating resistances obtained at various probe distances to zero [17,18], may be used in combination with the two-point probe technique to estimate the contact resistance. This approach, however, requires samples of several thicknesses which may be impractical.

A common method for evaluating σ_{tp} of highly filled CPCs is to apply a carbon paper between the electrodes and sample under a compressive load for improved electrical contact [19–23]. However, due to the roughness of both the composite and carbon paper, the measured σ_{tp} is dependent on the magnitude of the compressive load as well as type of carbon paper used which complicates comparison of results obtained by different laboratories [7]. It should be noted that Yao et al. [22] attempt to isolate the resistance of the CPC from the total resistance by measuring on CPCs with various thicknesses since their CPC resistance was proportional to the thickness. However, the method neglects the resistance of carbon papers and requires fabricating samples of various thicknesses which might be impractical. However, for thin plates relevant to bipolar plate applications, σ_{tp} may vary with plate thickness [24].

Other methods for reducing contact resistances during measurements of electrical properties do exist. For instance, Logakis et al. [25] sputtered gold on their samples to ensure good contact with their gold-plated electrodes. On the other hand, both Kunz et al. [9] and Liu et al. [26] applied a conductive silver paste between their CPCs and electrodes. However, these additional layers introduce contact resistances which should be quantified to obtain more accurate electrical properties of the samples of interest.

Alternatively, Sow et al. [27] used a highly filled CPC sandwiched between two current collectors with holes for sensing electrodes to directly contact the sample surface. This eliminated contact resistance between the sample and sensing electrodes. Yet, the equipotential planes close to the edge of the current collectors near the sensing electrodes bend, and thus potentials approaching the true surface potential of the sample are measured closest to the current collectors. This, however, requires fabrication of thin, concave electrodes. Q. Wei et al. [16] employed a coaxial structure to surround their thin film samples. The outer fixed-diameter probe was the source and the diameter of the inner sense probe was varied to allow the effect of source-sense probe distance to be screened. Simulation results showed the thinner the sample, the larger the voltage drop towards the sense probe with distance away from the source. Additionally, their experimental results showed higher electrical conductivities for samples measured with the largest diameter sensing probes since potentials closer to the source probe were measured. The strongest dependence of conductivity with sensing probe diameter was observed in relatively thin samples as expected from the simulation results. This may be problematic for highly filled CPCs in battery and fuel cell applications since they typically have thicknesses on the order of millimeters.

Instead, liquid metal contacts may be used as they are more tolerant to surface topography variations and may lower contact resistances [7]. Various liquid metals such as mercury and gallium-based alloys have been used as electrodes in microfluidic devices [28,29] and sensors [30,31]. The gallium-indium eutectic alloy (EGaIn), unlike mercury, is a non-toxic liquid metal, and due to its relatively high electrical conductivity (3.4×10^4 S cm^{-1}) and shear yielding rheology it may be used to form electrical contacts [32–34]. When exposed to air, EGaIn forms a nanometer thin oxide skin which does not significantly influence its bulk electrical conductivity, yet it enables EGaIn to be molded to form stable cones or droplets on surfaces [29,34–36]. After use, the liquid metal may be recovered and reused [29].

This paper proposes a new method for measuring σ_{tp} independent of applied pressure by applying EGaIn as moldable electrode contacts. Furthermore, we propose a route to correct the measured resistances for contributions from contact resistance, thus allowing us to report σ_{tp}-values which more closely resemble those of the composites. The accompanying setup is low-cost in terms of equipment, and it is uncomplicated to assemble. The resulting σ_{tp} obtained with this setup will be compared to the aforementioned carbon paper contact-method with partial compensation of contact resistances.

Materials and methods

Materials

A commercially available woven carbon paper (stamped into discs of diameter 39 mm) and blank, grinded polymer composite plates of thickness ~ 1.42 mm, consisting of a polyphenylene sulfide (PPS) matrix with graphite and carbon black filler particles, were obtained from Advent Technologies GmbH, Germany. These 'as received' plates were CNC-machined either into discs of 39 mm diameter or strips of width 15 mm and length 60 mm for through-plane and in-

plane electrical conductivity measurements, respectively. Gallium-indium eutectic alloy (75.5 wt.% Ga 24.5 wt.% In by weight, melting point 15.7 °C) was procured from Merck, Germany.

To study highly filled CPCs with various surface roughness, the above-mentioned 'as received' disc-shaped samples were wet-ground with SiC paper of grit sizes P120, P320 and P1200 (European FEPA P-grit sizes). Afterwards, the samples were rinsed with de-ionized water and ethanol and dried to ensure the surface was non-contaminated.

Microscopy

Scanning electron microcopy (SEM) images were acquired using a Zeiss EVO LS15 with an EHT of 15 kV. Surface topography was studied with a Zeiss Axio Imager. M2m light optical microscope (LOM). Reflected brightfield microscopy with a 50 × objective was used to obtain a minimum of 150 images per sample with a constant height between images. With the Zeiss ConfoMap ST software, the resulting three-dimensional stack was used to create a topographic map from which the arithmetic mean areal surface roughness (S_a) was calculated.

Electrical conductivity

In-plane electrical conductivity measurements were performed with a Tenma 72–2930 DC power supply and a Keysight 34465 A digital multimeter. In all two- and four-point probe measurements, a current of 1 A was forced through the samples. In the two-point probe measurement with EGaIn contacts, EGaIn was initially precoated on the sample (area $A_{EGaIn} = 0.13 \pm 0.01$ cm^2) before dispensing a droplet on the coated area. The distance between EGaIn contacts was $L = 4.1 \pm 0.1$ cm. With the four-point probe measurement, a distance between voltage-sensing probes of 2.0 cm was used. All reported in-plane electrical conductivities are based on six samples.

Through-plane electrical conductivity measurements were conducted with the same multimeter and power supply as the in-plane electrical conductivity measurements. For measurements with external pressure applied, the setup in Fig. 1a with gold-coated electrodes (Au) was used. Measurements were performed at three different pressures of 4.2 bar, 12.6 bar, and 20.1 bar and three currents (1 A, 5 A, and 10 A). Lastly, to compensate partly for contact resistances between carbon paper (CP) and Au-electrodes the method described in Ref. [20] was followed. The resistance measured from a single CP between the two Au-electrodes

$$R' = 2R_{Au} + R_{CP} + 2R_{Au/CP}, \quad (1)$$

With subscript '/' denoting an interface, was subtracted from the total resistance R of the setup in Fig. 1a

$$R = 2R_{Au} + 2R_{CP} + 2R_{Au/CP} + R_{sample} + 2R_{sample/CP}, \quad (2)$$

With 'sample' denoting the highly filled CPC. In these expressions, the internal resistances in the system were assumed negligible. This leaves the compensated value

$$R - R' = R_{sample} + R_{CP} + 2R_{sample/CP}. \quad (3)$$

The through-plane electrical conductivity measurements without external pressure were conducted with the setup schematically illustrated in Fig. 1b. A cotton swab was used to pre-coat EGaIn on a circular area of 0.15 ± 0.02 cm^2 on both surfaces of the sample. This was done to improve adhesion of the subsequently dispensed EGaIn droplet with the sample surface and to define the circular area through which current enters and exits the sample. Lastly, the four probes were pushed into the dispensed EGaIn droplets. The voltage was recorded at three different currents (1 A, 2.5 A, and 5 A), and the presented results are based on four to five samples. For

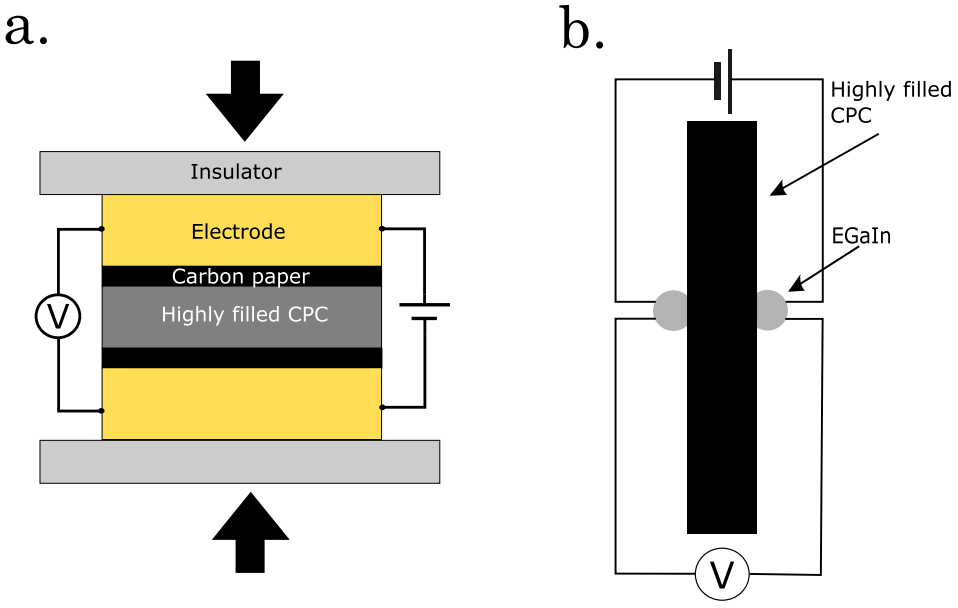

Fig. 1 – Schematic of setups for through-plane electrical conductivity measurements on highly filled conductive polymer composites (CPCs) with carbon paper (CP) (a) and gallium-indium eutectic (EGaIn) (b) as contact material. Arrows in (a) indicate the compressive load direction.

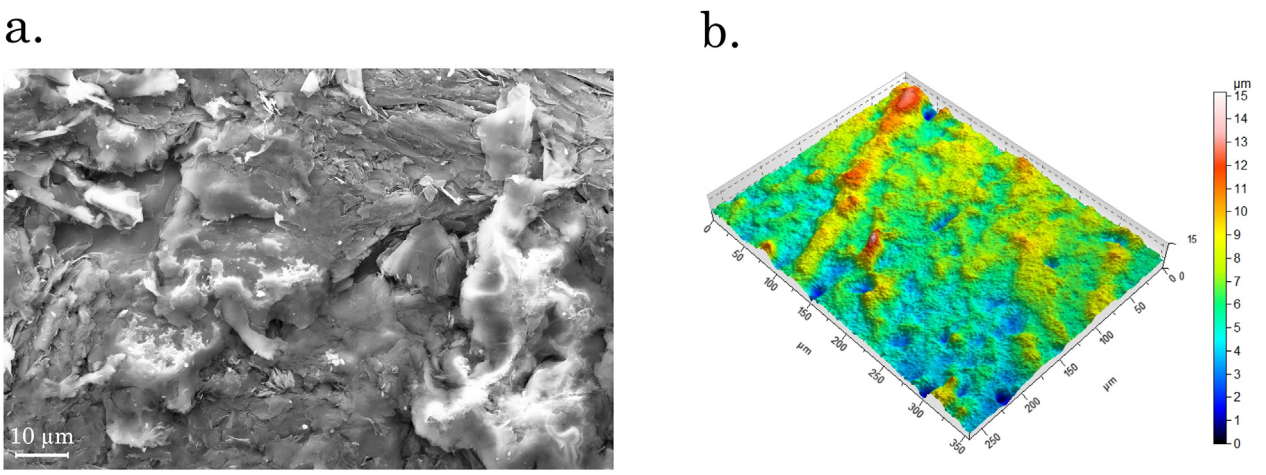

Fig. 2 – (a) Scanning electron microscopy image of an 'as-received' highly filled conductive polymer composite surface. The white spots are likely due to charging of the surface. (b) Surface topography map of an 'as-received' highly filled conductive polymer composite sample.

samples tested with both the CP and EGaIn contacts, the results are based on currents of 1 A as larger currents yielded identical conductivities.

Electrical conductivities (σ) were calculated based on the expression $\sigma = \frac{I \cdot L}{U \cdot \mathcal{A}}$, where I is the current, U potential difference, L separation between contacts parallel to the direction of current flow, and $\mathcal{A}$ the cross sectional area through which the current flows. In the case of EGaIn contacts, $\mathcal{A}$ was taken as the mean area of the two circular pre-coated EGaIn regions. With the four-point probe measurement, L was taken as the distance between voltage-sensing probes.

Results and discussion

Surface roughness

The roughness of the sample surfaces was evaluated both by SEM and LOM. The resulting images of the 'as received' highly filled CPC surface are presented in Fig. 2, respectively.

Although no quantitative height information can be extracted from the SEM image, Fig. 2a shows a rough, flaky surface. From the topographic map, Fig. 2b, a height variation on the scale of several micrometers is observed, resulting in $S_a = 1.3 \pm 0.1$ µm. The roughness and observed topography will result in a lower true contact area between CP and highly filled CPC and, thus, increase the contact resistance.

The wet-grinding procedure produced the mean areal surface roughness presented in Table 1. As can be observed, the roughness of the grinded 'as received' samples is in between that of the samples wet-grinded with P320 and P1200 SiC paper.

Liquid metal contacts

To validate the use of EGaIn as contact material for the polymer composites, measurements were conducted with both the two- and four-point probe techniques to measure in-plane electrical conductivities (σ_{ip}). A disadvantage of the two-point probe technique (2-PP in Fig. 3) is the contact resistance between sample and electrical contacts which becomes increasingly important as the electrical conductivity of the sample increases. In the two-point probe technique with EGaIn contacts (2-PP w. EGaIn in Fig. 3) the sample is precoated with two EGaIn contacts and both pairs of source and sensing electrodes are introduced in their respective EGaIn contacts. Hence, the measured voltage drop will include a contribution from the contact resistance between EGaIn and sample. This contact resistance is, however, eliminated with the four-point probe technique [18] (4-PP in Fig. 3) used to obtain the inherent in-plane electrical conductivity of the sample.

By comparing σ_{ip} from the 2-PP and 2-PP w. EGaIn techniques in Fig. 3, a 42 times improvement in σ_{ip} is noticed. It is likewise interesting that σ_{ip} from 2-PP w. EGaIn and 4-PP techniques deviate by only 17% with the lower σ_{ip} measured by the former technique being primarily due to contact resistances between EGaIn and sample.

Writing out the contributions to the total resistance measured with the 2-PP w. EGaIn technique results in $R_{2-PP\ w.\ EGaIn} = R_{sample} + 2R_{EGaIn/sample}$ with the last term accounting for the voltage drop associated with the contact resistance between EGaIn and sample. Here it has been assumed that the bulk resistance of EGaIn and any contact resistance between sensing electrode and EGaIn may be neglected due to the aforementioned high electrical

Table 1 – Arithmetic mean areal surface roughness (S_a) for the samples used to evaluate through-plane electrical conductivities.

Grit size	S_a [μm]
P120	6.5 ± 2.0
P320	3.0 ± 0.3
P1200	0.65 ± 0.07
'As received'	1.3 ± 0.1

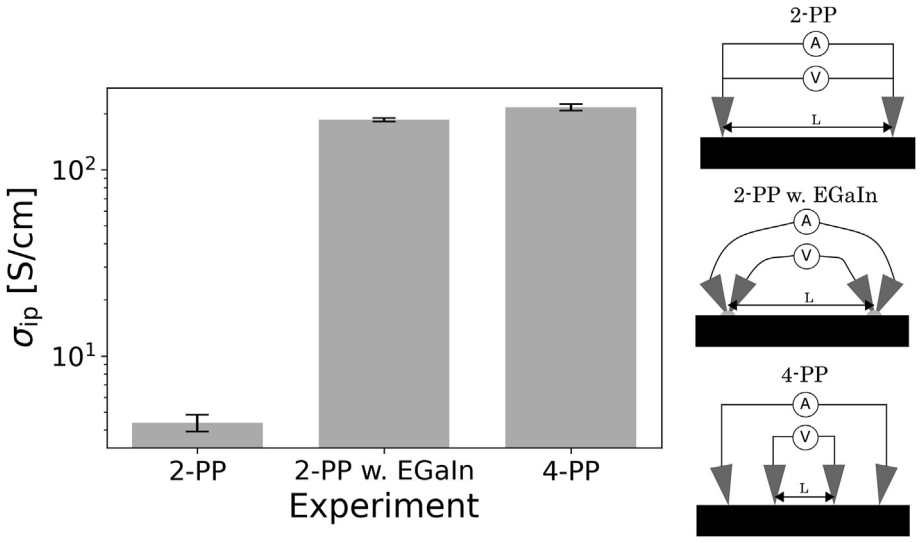

Fig. 3 – In-plane electrical conductivities (σ_{ip}) of 'as received' highly filled conductive polymer composites (CPCs) measured with the illustrated two- and four-point probe techniques at a current of 1 A. Error bars indicate ± one standard deviation. 2-PP: two-point probe. 2-PP w. EGaIn: two-point probe with EGaIn contacts. 4-PP: four-point probe. *L*: distance between sensing probes. Please see Section Materials and methods for a description of the samples and setup.

conductivity of EGaIn $(>10^4$ S cm$^{-1})$ and good wetting of the metal electrode by EGaIn. Finally, in the 4-PP technique, where voltage-measuring electrodes are situated on the sample of interest, it may be assumed that the measured resistance equals the sample resistance, i.e., $R_{4-PP} = R_{sample}$.

The above considerations may be used to obtain an estimate of the areal contact resistance $(\mathcal{R}_{EGaIn/sample})$ between EGaIn and sample by subtracting the sample resistance from the resistance measured by the 2-PP w. EGaIn technique, i.e., $\mathcal{R}_{EGaIn/sample} = R_{EGaIn/sample} \cdot 2A_{EGaIn} = (R_{2-PP\ w.EGaIn} - R_{4-PP}) \cdot A_{EGaIn}$. Applying this to the investigated samples result in $\mathcal{R}_{EGaIn/sample} = 0.85 \pm 0.12$ mΩ cm^2. As a comparison, this value is almost 30 times lower than the contact resistivity of an unpolished BMC bipolar plate surface and a Toray carbon paper at 6.5 MPa [20], and nine times lower than between a Toray TGPH-060 gas diffusion layer and a polyvinylidene fluoride/graphite (35 wt.%)/multi-walled carbon nanotube (5 wt.%) composite [23]. A recent target for the contact resistance between bipolar plate and gas diffusion layer set by the US Department of Energy is <10 mΩ cm^2 [37], with several authors having reported contact resistances in fulfillment of this target and down to roughly 2 mΩ cm^2 [27,38–40]. Our estimated areal contact resistance between EGaIn and sample will be applied to the through-plane electrical conductivity results.

Through-plane electrical conductivity

The measured through-plane electrical conductivities obtained with either CPs or EGaIn as contact material are presented in Fig. 4a. With CPs, the compensated σ_{tp} (see Eq. (3)) is seen to almost double from 10 S cm^{-1} at 4.2 bar to 19 S cm^{-1} at 20.1 bar. The conductivity increase with pressure results mainly from the decrease in interfacial resistance between the CP and sample due to an increased effective contact area caused by deformation of surface asperities on the CP and sample surfaces [27]. Observing the discrepancy between the compensated and uncompensated σ_{tp}, a decreased relative deviation from 42% at 4.2 bar to 27% at 20.1 bar is noted. To some degree, this is influenced by an increased effective contact area between CP and electrodes, but the resistivity of CPs also depend on compressive pressure due to the formation of fiber cracks and a resulting alteration of conductive pathways [41].

Fig. 4a indicates an up to six times higher measured σ_{tp} using EGaIn as contact material in contrast to CP contacts. Besides the comparatively higher conductivity of EGaIn compared to CP, this could be due to EGaIn more easily conforming to the surface topography of the sample than the solid CP material, thereby increasing the effective contact area and hence reducing the contact resistance [7].

Since the contact resistance between EGaIn and highly filled CPC sample is normal to the sample surface, and the difference between the approach in Fig. 1b and the 2-PP w. EGaIn technique lies solely in the current flow direction through the sample, the areal contact resistance $\mathcal{R}_{EGaIn/sample}$ from in-plane electrical conductivity measurements can be used to compensate for contact resistance in σ_{tp}-measurements. Hence, $\mathcal{R}_{EGaIn/sample}$ is multiplied by the area of EGaIn contacts from σ_{tp}-measurements to obtain a representative contact resistance contribution to σ_{tp}. Subtracting this resistance from the total resistance measured with the setup in Fig. 1b for 'as received' samples results in $\sigma_{tp}^{comp} = 76 \pm 9$ S cm^{-1}, a value 46% larger than the uncompensated $\sigma_{tp}^{uncomp} = 52 \pm 4$ S cm^{-1}, Fig. 4a.

Fig. 4b shows the variation of σ_{tp} with surface roughness of the highly filled CPC surface. Overlap of σ_{tp} at all three roughness-values is observed. The lower values of σ_{tp} obtained for surfaces with $S_a = 6.5 \pm 2.0$ μm suggest a greater contact resistance due to poorer wetting of the rough surface.

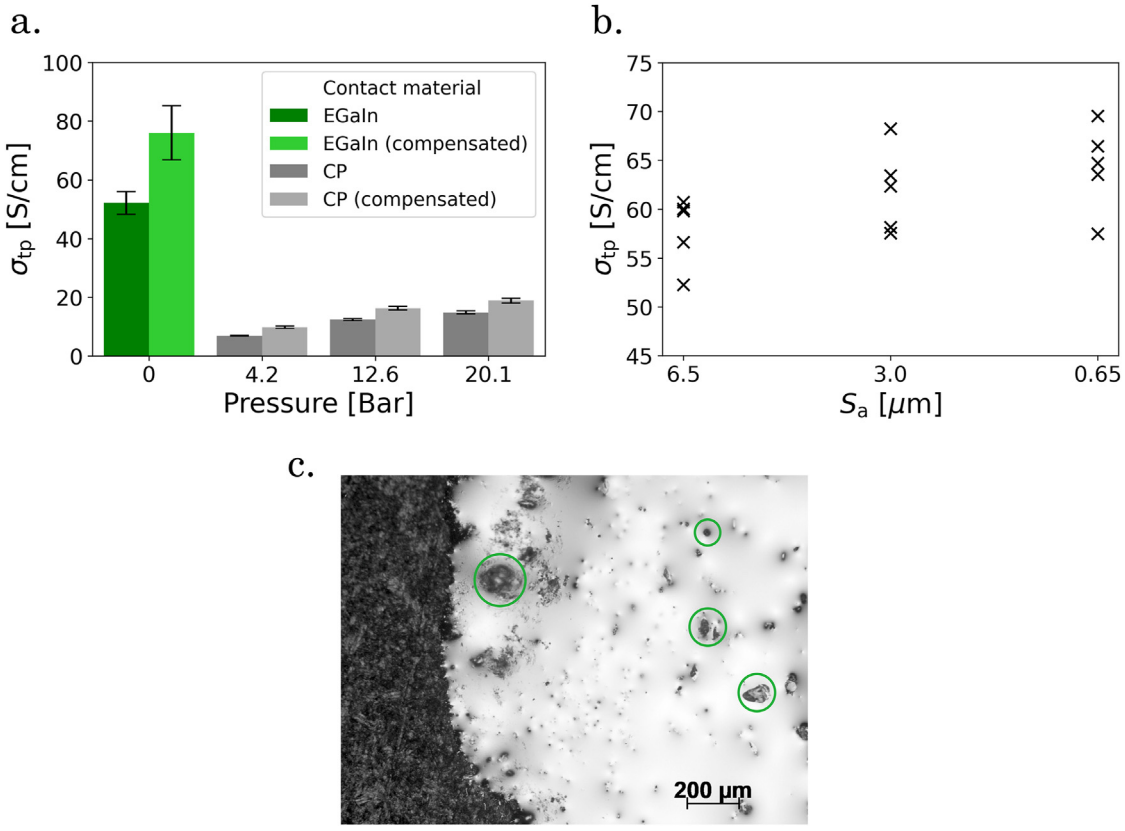

Fig. 4 – (a) Measured through-plane electrical conductivities (σ_{tp}) of 'as received' highly filled CPCs at a current of 1 A. Reported results are based on four and three samples for the EGaIn-method and carbon paper-method (CP), respectively. Compensated values with CP contacts are based on Eq. (3) while with EGaIn contacts, compensated values are found by subtracting the areal contact resistance between EGaIn and highly filled CPC sample from the measured resistance. Error bars indicate ± one standard deviation. (b) Measured σ_{tp} at a current of 1 A for highly filled CPCs of various arithmetic mean areal surface roughness (S_a). The sample surface roughness and corresponding mean conductivities are: $S_a = 6.5 \pm 2.0$ µm and $\sigma_{tp} = 58 \pm 3$ S cm^{-1}; $S_a = 3.0 \pm 0.3$ µm and $\sigma_{tp} = 62 \pm 4$ S cm^{-1}; $S_a = 0.65 \pm 0.07$ µm and $\sigma_{tp} = 64 \pm 4$ S cm^{-1}. Five different samples were tested at each surface roughness. (c) Light optical microscopy image of an 'as received' highly filled CPC (dark grey) pre-coated with EGaIn (silver). The dark spots, some of which have been highlighted by green circles, are regions not wetted by EGaIn. (For interpretation of the references to colour in this figure legend, the reader is referred to the Web version of this article.)

As can be seen in Fig. 4c, precoating with EGaIn does not ensure uniform wetting of the substrate. It can be expected that the lower surface energy of PPS compared to the conductive fillers causes EGaIn to preferably wet the latter. Thus, returning to the SEM image, Fig. 2, the white spots could indicate local areas of PPS at the surface which may hinder uniform wetting of the substrate. Additionally, with a head diameter on the order of millimeters, the cotton swabs used for precoating the substrate are expected to have more difficulty distributing the EGaIn in valleys of relatively rough surfaces, thereby offering a possible explanation for the trend observed in Fig. 4b. So, the proposed method appears less suited to study rough surfaces. Yet, highly filled CPCs for fuel cell bipolar plate applications in general benefit from possessing smooth surfaces due to lower contact resistance and, hence, lower voltage drop [42]. Thus, the proposed approach may be a viable alternative to characterize σ_{tp} for said applications.

Conclusions

Measurements of through-plane electrical conductivities (σ_{tp}) on highly filled conductive polymer composites using either (i) carbon papers as contact material with externally applied pressure, or (ii) a liquid gallium-indium eutectic alloy (EGaIn), result in higher measured σ_{tp} by adopting the latter method. Thus, with EGaIn as electrical contacts a decrease in contact resistance is observed, resulting in σ_{tp}-values more closely resembling those of the composites. Furthermore, as the method of EGaIn as contact material is pressure-independent, comparison of experimental results between laboratories is expected to become more straightforward.

It would be fruitful to investigate the applicability of alternative metals to EGaIn that, similarly, are liquid at room temperature, e.g., GaInSn eutectic alloy ('Galinstan') [32]. An alternative approach could be to use conductive colloidal gels

with conductive granular fillers such that the contacts possess a yield stress sufficiently high to allow forming stable contacts and prevent sedimentation of the granular fillers.

Declaration of competing interest

The authors declare that they have no known competing financial interests or personal relationships that could have appeared to influence the work reported in this paper.

Acknowledgements

This work was supported in part by Advent Technologies A/S and a grant from the Industrial PhD programme, Innovation Fund Denmark, project 8053-00063B.

REFERENCES

[1] Song Y, Zhang C, Ling C-Y, Han M, Yong R-Y, Sun D, et al. Review on current research of materials, fabrication and application for bipolar plate in proton exchange membrane fuel cell. Int J Hydrogen Energy 2020;45:29832–47. https://doi.org/10.1016/j.ijhydene.2019.07.231 [progress in Fuel Cells].

[2] Naji A, Krause B, Potschke P, Ameli A. Hybrid conductive filler/polycarbonate composites with enhanced electrical and thermal conductivities for bipolar plate applications, Polym. Composer 2019;40:3189–98. https://doi.org/10.1002/pc.25169.

[3] Duan Z, Qu Z, Ren Q, Zhang J. Review of bipolar plate in redox flow batteries: materials, structures, and manufacturing. Electrochem Energy Rev 2021;4:718–56. https://doi.org/10.1007/s41918-021-00108-4.

[4] Heinzel A, Mahlendorf F, Niemzig O, Kreuz C. Injection moulded low cost bipolar plates for PEM fuel cells. J Power Sources 2004;131:35–40. https://doi.org/10.1016/j.jpowsour.2004.01.014.

[5] Antunes RA, de Oliveira MCL, Ett G, Ett V. Carbon materials in composite bipolar plates for polymer electrolyte membrane fuel cells: a review of the main challenges to improve electrical performance. J Power Sources 2011;196:2945–61. https://doi.org/10.1016/j.jpowsour.2010.12.041.

[6] Saadat N, Dhakal HN, Tjong J, Jaffer S, Yang W, Sain M. Recent advances and future perspective of carbon materials for fuel cell. Renew Sustain Energy Rev 2021;138:110535. https://doi.org/10.1016/j.rser.2020.110535.

[7] Shaigan N, Yuan X-Z, Girard F, Fatih K, Robertson M. Standardized testing framework for quality control of fuel cell bipolar plates. J Power Sources 2021;482:228972. https://doi.org/10.1016/j.jpowsour.2020.228972.

[8] Radzuan NAM, Sulong AB, Somalu MR, Abdullah AT, Husaini T, Rosli RE, et al. Fibre orientation effect on polypropylene/milled carbon fiber composites in the presence of carbon nanotubes or graphene as a secondary filler: application on PEM fuel cell bipolar plate. Int J Hydrogen Energy 2019;44:30618–26. https://doi.org/10.1016/j.ijhydene.2019.01.063.

[9] Kunz K, Krause B, Kretzschmar B, Juhasz L, Kobsch O, Jenschke W, et al. Direction dependent electrical conductivity of polymer/carbon filler composites. Polymers 2019;11:591. https://doi.org/10.3390/polym11040591.

[10] Lee MH, Kim HY, Oh SM, Kim BC, Bang D, Han JT, et al. Structural optimization of graphite for high-performance fluorinated ethylene–propylene composites as bipolar plates. Int J Hydrogen Energy 2018;43:21918–27. https://doi.org/10.1016/j.ijhydene.2018.09.104.

[11] Jeong KI, Oh J, Song SA, Lee D, Lee DG, Kim SS. A review of composite bipolar plates in proton exchange membrane fuel cells: electrical properties and gas permeability. Compos Struct 2021;262:113617. https://doi.org/10.1016/j.compstruct.2021.113617.

[12] San FGB, Tekin G. A review of thermoplastic composites for bipolar plate applications. Int J Energy Res 2013;37:283–309. https://doi.org/10.1002/er.3005.

[13] Cunningham BD, Huang J, Baird DG. Development of bipolar plates for fuel cells form graphite filled wet-lay material and a thermoplastic laminate skin layer. J Power Sources 2007;165:764–73. https://doi.org/10.1016/j.jpowsour.2006.12.035.

[14] Darıcık F, Topcu A, Aydın K, Çelik S. Carbon nanotube (cnt) modified carbon fiber/epoxy composite plates for the pem fuel cell bipolar plate application. Int J Hydrogen Energy 2022. https://doi.org/10.1016/j.ijhydene.2022.09.297.

[15] Timsit R. Electrical contact resistance: properties of stationary interfaces. IEEE Trans Compon Packag Technol 1999;22:85–98. https://doi.org/10.1109/6144.759357.

[16] Wei Q, Suga H, Ikeda I, Mukaida M, Kirihara K, Naitoh Y, et al. An accurate method to determine the through-plane electrical conductivity and to study transport properties in film samples. Org Electron 2016;38:264–70. https://doi.org/10.1016/j.orgel.2016.08.030.

[17] Kokabu T, Inoue S, Matsumura Y. Estimation of adsorption energy for water molecules on a multi-walled carbon nanotube thin film by measuring electric resistance. AIP Adv 2016;6:115212. https://doi.org/10.1063/1.4967784.

[18] Rojo MM, Manzano CV, Granados D, Osorio MR, Borca-Tasciuc T, Martin-Gonzalez M. High electrical conductivity in out of plane direction of electrodeposited Bi_2Te_3 films. AIP Adv 2015;5:087142. https://doi.org/10.1063/1.4928863.

[19] Cunningham N, Lefevre M, Lebrun G, Dodelet J-P. Measuring the through-plane electrical resistivity of bipolar plates (apparatus and methods). J Power Sources 2005;143:93–102. https://doi.org/10.1016/j.jpowsour.2004.11.062.

[20] Avasarala B, Haldar P. Effect of surface roughness of composite bipolar plates on the contact resistance of a proton exchange membrane fuel cell. J Power Sources 2009;188:225–9. https://doi.org/10.1016/j.jpowsour.2008.11.063.

[21] Dhakate SR, Sharma S, Chauhan N, Seth RK, Mathur RB. CNTs nanostructuring effect on the properties of graphite composite bipolar plate. Int J Hydrogen Energy 2010;35:4195–200. https://doi.org/10.1016/j.ijhydene.2010.02.072.

[22] Yao K, Adams D, Hao A, Zheng JP, Liang Z, Nguyen N. Highly conductive and strong graphite-phenolic resin composite for bipolar plate applications. Energy Fuels 2017;31:14320–31. https://doi.org/10.1021/acs.energyfuels.7b02678.

[23] Hu B, Chang F-L, Xiang L-Y, He G-J, Cao X-W, Yin X-C. High performance polyvinylidene fluoride/graphite/multi-walled carbon nanotubes composite bipolar plate for pemfc with segregated conductive networks. Int J Hydrogen Energy 2021;46:25666–76. https://doi.org/10.1016/j.ijhydene.2021.05.081.

[24] Bühler R, Thommen M, Le Canut J-M, Weber J-F, Rytka C, Tsotra P. Highly conductive polypropylene-based composites for bipolar plates for polymer electrolyte membrane fuel cells. Fuel Cell 2021;21:155–63. https://doi.org/10.1002/fuce.201900232.

[25] Logakis E, Pandis C, Peoglos V, Pissis P, Pionteck J, Pötschke P, et al. Electrical/dielectric properties and conduction mechanism in melt processed polyamide/multi-walled carbon nanotubes composites. Polymer 2009;50:5103–11. https://doi.org/10.1016/j.polymer.2009.08.038.
[26] Liu H, Gao J, Huang W, Dai K, Zheng G, Liu C, et al. Electrically conductive strain sensing polyurethane nanocomposites with synergistic carbon nanotubes and graphene bifillers. Nanoscale 2016;8:12977. https://doi.org/10.1039/c6nr02216b.
[27] Sow PK, Prass S, Kalisvaart P, Merida W. Deconvolution of electrical contact and bulk resistance of gas diffusion layers for fuel cell applications. Int J Hydrogen Energy 2015;40:2850–61. https://doi.org/10.1016/j.ijhydene.2014.12.110.
[28] Ota H, Chen K, Lin Y, Kiriya D, Shiraki H, Yu Z, et al. Highly deformable liquid-state heterojunction sensors. Nat Commun 2014;5:5032. https://doi.org/10.1038/ncomms6032.
[29] Khoshmanesh K, Tang S-Y, Zhu JY, Schaefer S, Mitchell A, Kalantar-zadeh K, et al. Liquid metal enabled microfluidics. Lab Chip 2017;17:974. https://doi.org/10.1039/c7lc00046d.
[30] Zhou X, Zhang R, Li L, Zhang L, Liu B, Deng Z, et al. A liquid metal based capacitive soft pressure microsensor. Lab Chip 2019;19:807. https://doi.org/10.1039/c8lc01357h.
[31] Zhang R, Ye Z, Gao M, Gao C, Zhang X, Li L, et al. Liquid metal electrode-enabled flexible microdroplet sensor. Lab Chip 2020;20:496. https://doi.org/10.1039/c9lc00995g.
[32] Scharmann F, Cherkashinin G, Breternitz V, Knedlik C, Hartung G, Weber T, et al. Viscosity effect on GaInSn studied by XPS. Surf Interface Anal 2004;36:981–5. https://doi.org/10.1002/sia.1817.
[33] Kramer RK, Boley JW, Stone HA, Weaver JC, Wood RJ. Effect of microtextured surface topography on the wetting behavior of eutectic gallium-indium alloys. Langmuir 2013;30:533–9. https://doi.org/10.1021/la404356r.
[34] Douvogianni E, Qiu X, Qiu L, Jahani F, Kooistra FB, Hummelen JC, et al. Soft nondamaging contacts formed from eutectic Ga-In for the accurate determination of dielectric constants of organic materials. Chem Mater 2018;30:5527–33. https://doi.org/10.1021/acs.chemmater.8b02212.
[35] Dickey MD, Chiechi RC, Larsen RJ, Weiss EA, Weitz DA, Whitesides GM. Eutectic gallium-indium (EGaIn): a liquid metal alloy for the formation of stable structures in microchannels at room temperature. Adv Funct Mater 2008;18:1097–104. https://doi.org/10.1002/adfm.200701216.
[36] Kim D, Thissen P, Viner G, Lee D-W, Choi W, Chabal YJ, et al. Recovery of nonwetting characteristics by surface modification of gallium-based liquid metal droplets using hydrochloric acid vapor. ACS Appl Mater Interfaces 2013;5:179–85. https://doi.org/10.1021/am302357t.
[37] Qiu D, Peng L, Yi P, Lehnert W, Lai X. Review on proton exchange membrane fuel cell stack assembly: quality evaluation, assembly method, contact behavior and process design. Renew Sustain Energy Rev 2021;152:111660. https://doi.org/10.1016/j.rser.2021.111660.
[38] Yi P, Peng L, Zhou T, Wu H, Lai X. Cr–n–c multilayer film on 316l stainless steel as bipolar plates for proton exchange membrane fuel cells using closed field unbalanced magnetron sputter ion plating. Int J Hydrogen Energy 2013;38:1535–43. https://doi.org/10.1016/j.ijhydene.2012.11.030. 2011 Zing International Hydrogen and Fuel Cells Conference: from Nanomaterials to Demonstrators.
[39] Yi P, Zhang D, Qiu D, Peng L, Lai X. Carbon-based coatings for metallic bipolar plates used in proton exchange membrane fuel cells. Int J Hydrogen Energy 2019;44:6813–43. https://doi.org/10.1016/j.ijhydene.2019.01.176.
[40] Xu Z, Qiu D, Yi P, Peng L, Lai X. Towards mass applications: a review on the challenges and developments in metallic bipolar plates for pemfc. Prog Nat Sci: Mater Int 2020;30:815–24. https://doi.org/10.1016/j.pnsc.2020.10.015.
[41] Qiu D, Janßen H, Peng L, Irmscher P, Lai X, Lehnert W. Electrical resistance and microstructure of typical gas diffusion layers for proton exchange membrane fuel cell under compression. Appl Energy 2018;231:127–37. https://doi.org/10.1016/j.apenergy.2018.09.117.
[42] San FGB, Okur O. The effect of compression molding parameters on the electrical and physical properties of polymer composite bipolar plates. Int J Hydrogen Energy 2017;42:23054–69. https://doi.org/10.1016/j.ijhydene.2017.07.175.